Available online at www.sciencedirect.com
ScienceDirect
ELSEVIER
Surface Science 600 (2006) 4870–4877
SURFACE SCIENCE
www.elsevier.com/locate/susc

Hydroxylated α-Al_2O_3 (0001) surfaces and metal/α-Al_2O_3 (0001) interfaces

Qiang Fu [a,b], Thomas Wagner [a,*,1], Manfred Rühle [a]

[a] *Max-Planck-Institut für Metallforschung, Heisenbergstrasse 3, D-70569 Stuttgart, Germany*
[b] *State Key Laboratory of Catalysis, Dalian Institute of Chemical Physics, The Chinese Academy of Sciences, Zhongshan Road 457, Dalian 116023, PR China*

Received 27 February 2006; accepted for publication 9 August 2006
Available online 28 August 2006

Abstract

X-ray photoelectron spectroscopy was applied to study the hydroxylation of α-Al_2O_3 (0001) surfaces and the stability of surface OH groups. The evolution of interfacial chemistry of the α-Al_2O_3 (0001) surfaces and metal/α-Al_2O_3 (0001) interfaces are well illustrated via modifications of the surface O1s spectra. Clean hydroxylated surfaces are obtained through water- and oxygen plasma treatment at room temperature. The surface OH groups of the hydroxylated surface are very sensitive to electron beam illumination, Ar^+ sputtering, UHV heating, and adsorption of reactive metals. The transformation of a hydroxylated surface to an Al-terminated surface occurs by high temperature annealing or Al deposition.
© 2006 Elsevier B.V. All rights reserved.

Keywords: X-ray photoelectron spectroscopy; Molecular beam epitaxy; Metallic films; Aluminum oxide; Metal-oxide interfaces; Surface chemical reactions

1. Introduction

Metal film growth and the formation of well defined interfaces depend sensitively on the crystallographic and electronic structure of the substrate surface. Alumina surfaces are one of the most extensively studied surfaces [1,2]. They are very important as thin-film substrates and catalyst supports. In particular, the crystallographic simple and energetically stable (0001) surface of corundum alumina (α-Al_2O_3: sapphire) offers a good playground for fundamental studies concerning the influence of surface properties (e.g., crystallographic- and electronic structure) on the formation of interfaces.

The unit cell of bulk α-Al_2O_3 can be described as a hexagonal unit cell containing six formula units of Al_2O_3 [3]. This unit cell consists of six close-packed hexagonal O layers. Al layers, which are not coplanar but buckled, are placed between these O layers. The Al ions are placed in 2/3 of the octahedral vacancies. All the ions are stacked along the *c*-axis of the unit cell in a sequence *R*-$AlAlO_3$-*R* (*R*: continuing sequence in the bulk). For bulk truncated α-Al_2O_3 (0001) surfaces there exist, from a geometrical standpoint, three different terminations (e.g., see Fig. 1 in Ref. 4): O layer termination (O_3AlAl-*R*), single Al layer termination (AlO_3Al-*R*), and double Al layer termination ($AlAlO_3$-*R*) [4–6]. The 3 surfaces possess different thermodynamic stabilities [6–10].

The O layer terminated surface has a large surface dipole moment and surface dangling bonds. Therefore, this surface is energetically unstable under almost all environmental conditions [6]. The O layer termination was observed experimentally only by Toofan and Watson who reported a mixture of 2:1 O/Al-terminated surface domains [11].

The single Al layer terminated surface is generally accepted to be the most stable unreconstructed α-Al_2O_3

* Corresponding author. Tel.: +49 711 689 1429; fax: +49 711 689 1472.
E-mail addresses: qfu@dicp.ac.cn (Q. Fu), t.wagner@fkf.mpg.de (T. Wagner).
[1] Present address: Max-Planck-Institut für Festkörperforschung, Heisenbergstrasse 1, D-70569 Stuttgart, Germany.

0039-6028/$ - see front matter © 2006 Elsevier B.V. All rights reserved.
doi:10.1016/j.susc.2006.08.008

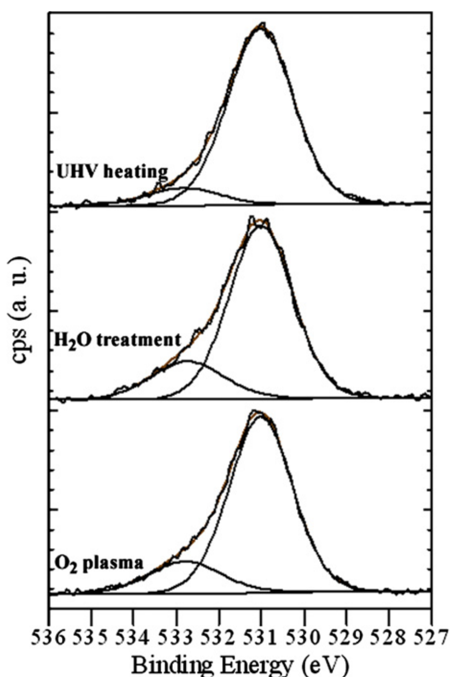

Fig. 1. O1s XPS spectra of the α-Al_2O_3 (0001) surface after UHV heating at 900 °C for 2 h, H_2O-, and O_2 plasma treatment at RT, respectively.

(0001) surface [4–19]. The surface is non-polar. Moreover, surface Al atoms strongly relax inward so that they are almost coplanar with respect to the second O layer. The relaxation is accompanied by a rehybridization of surface Al atoms to an sp^2 orbital configuration, which significantly stabilizes the surfaces via charge autocompensation [6]. The surface relaxation was calculated with density functional theory (DFT) to be about −85%, e.g., −85% [7], −82% [14,15], −87% [16], −86% [6,17], and −83% [19]. However, experimentally observed relaxations were smaller, ranging from −51% to −63% [4,5,13]. These results were obtained by X-ray diffraction (XRD) [5], low energy electron diffraction (LEED) [4], and ion scattering [13], respectively.

The (1 × 1) surface may be subjected to reconstructions in cases of O desorption or Al deposition onto the surface [20–24]. Such reconstructions are favored by energetical reasons. XRD and LEED investigations have revealed a $(\sqrt{31} \times \sqrt{31})\, R \pm 9°$ reconstruction on α-Al_2O_3 (0001) surfaces heated in ultrahigh vacuum (UHV) at $T > 1200$ °C [21–23] or covered by Al [23,24]. The reconstructed surfaces were suggested to be terminated by a double Al layer, which contains hexagonal surface domains with Al (111) structure [20,21]. Such a structure has been directly imaged using dynamic-mode scanning force microscopy (SFM) by Barth and Reichling [20].

Hydroxylation of clean α-Al_2O_3 (0001) surfaces may result in further lowering of the energies of these surfaces [6–8,25]. Thus, the above O- and Al-terminated surfaces are expected to be reactive to water. Theoretically, *ab initio* calculation revealed that molecularly adsorbed water on Al-terminated surfaces is metastable and dissociates readily. The H_2O dissociative reactions produce two types of surface OH groups: $O_{ads}H$ and O_sH (O_{ads}: water oxygen; O_s: surface oxygen) [14,15,26]. Experiments confirmed the existence of OH-terminated α-Al_2O_3 (0001) surfaces by various techniques, e.g., SFM [20], XRD [27], thermal desorption [28,29], electron-energy loss spectroscopy (EELS) [30], and X-ray photoelectron spectroscopy (XPS) [31–36]. The surfaces in these studies were simply obtained via exposure to water or air.

As pointed out above, the α-Al_2O_3 (0001) surface exhibits four basic varieties of surface terminations, including O layer termination, single Al layer termination, double Al layer termination, and OH termination. Each of these surfaces has a unique stoichiometry, crystallographic and electronic structure, etc. The different surface terminations and properties deliberately depend on the surface treatment and can be manipulated by the surface preparation process. The different surface properties will significantly affect the formation of metal/alumina interfaces, for example, nucleation and growth of metal overlayers, interfacial bonding, and thus interfacial energy [32–43]. Among the different possible surfaces, the hydroxylated α-Al_2O_3 surface is of special importance. First of all, alumina surfaces are quite often covered by water or exposed, of course, to air during handling. Therefore, OH groups will always be present on the surfaces in case of no further special surface treatment. On the other hand, surface OH groups are critical for metal deposition. Hydroxylated surfaces are expected to exhibit higher reactivity to metals than clean Al-terminated surfaces [27,32–37]. Theoretical work [34,38] predicted that the reactions of Co and Cu with surface OH groups are exothermic. The interfacial reactions lead, instead of island growth, to the technologically important 2-D film growth and the oxidation of the metal in the initial stage of nucleation. In general, the strong interaction between metal adatoms and surface OH groups significantly changes the interfacial bonding and solid state wetting behavior [32–38]. Therefore, fully understanding and well controlling of the hydroxylated α-Al_2O_3 (0001) surface can contribute much to the elucidation of the nature of metal/alumina interfaces.

In the present paper, we concentrate on the hydroxylated sapphire (0001) surface (sapphire basal plane). Angle-resolved XPS was used to study the interfacial chemistry at the OH-terminated α-Al_2O_3 (0001) surfaces and interaction with various metals. In particular, we addressed the following points: preparation of the OH-terminated surfaces, the stability of the surface OH groups to different treatments, and the interaction between metal adatoms and OH groups. A critical comparison of our results to previous experimental and theoretical data will be given in Section 3.

2. Experimental

Single crystal α-Al_2O_3 (0001) platelets (10 mm × 10 mm × 0.5 mm, polished on one side, with a deliberate

surface miscut of 0.1°) were used as substrates (Crystal GmbH, Berlin). After cleaning in acetone the samples were placed into a multi-chamber UHV molecular beam epitaxy (MBE) system (Metal 600, DCA Instruments). A normal surface preparation process within the MBE system was performed as follows: (i) UHV heating at 900 °C for 1 h, (ii) 200 eV Ar^+ sputtering for 10 min (beam current: 5 mA), and (iii) a second UHV heating at 900 °C for 2 h. This procedure results in clean, well-defined, and unreconstructed surfaces as confirmed by in-situ Auger electron spectroscopy (AES) and reflection high-energy electron diffraction (RHEED) measurements [44]. In the following, this UHV annealed surface will be called *normal surface*.

Subsequently, the hydroxylation was performed by exposing the normal surface to double-deionized water drops in the load-lock of the UHV system. During this procedure the load-lock was subjected to flowing N_2. Afterwards, the water-exposed surfaces were treated at room temperature (RT) in oxygen plasma (250 W, 10 min), generated by an electron cyclotron resonance (ECR) device (Oxford instruments). The water treated surface will be called *hydroxylated surface*.

The annealing and metal deposition was carried out in the growth chamber of the UHV system. Al and Co were deposited by electron beam evaporators, and Cu was evaporated from an effusion cell. The nominal thicknesses of the metal layers were monitored by a quartz crystal balance. Heating was conducted using a BN covered graphite resistance heater. The temperature of the samples was measured by a calibrated W–Re thermocouple. The growth chamber was equipped with RHEED (Staib Instruments, 30 keV), which was applied to investigate the sapphire surface structure and the metal film growth.

Surface analysis was performed in the analysis chamber of the UHV system, consisting of XPS, AES, and scanning probe microscopy. The XPS measurements were carried out with an Mg Kα X-ray source ($E_0 = 1253.6$ eV, 400 W) and a hemispherical energy analyzer (SPECS PHOIBOS 150) at a pass energy of 20 eV. Due to the small acceptance angle (<2° in case of small aperture size) of the analyzer, angle-resolved measurement is possible. Typically, XPS spectra were collected at two geometries: grazing detection (at 70° off the normal to the sample surface) and normal detection (at 0° off the normal to the surface). All XPS data shown below were recorded at grazing detection angle to increase the surface sensitivity. The core level spectra, e.g., O1s, were fitted using Gaussian–Lorentzian peaks after subtracting a Shirley background [45]. We observed strong charging effects during XPS measurements. Therefore, the line shape rather than the line position of O1s spectra was used to characterize the chemical state of surface oxygen. However, in order to compare the line shape of different spectra, all O1s spectra were normalized and their main peak positions were calibrated to the same binding energy (BE), 531.0 eV [46]. The change in surface chemistry was mainly derived from the evolution of line shape of the spectra. AES signals were excited by an electron gun (SPECS, EQ 22/35) and recorded using the same energy analyzer. The electron gun was additionally used to study the influence of the primary electron beam on the surface composition of the hydroxylated surfaces.

3. Results and discussion

3.1. The hydroxylation of Al_2O_3 (0001) surfaces

The hydroxylation of the surface was stepwise performed by the normal UHV heating process, exposure to H_2O, and O_2 plasma at RT. The O1s spectra recorded from the differently treated surfaces are shown in Fig. 1. All the spectra are asymmetric with a tail at higher BE and can be well fitted by two peaks. The full width at half maximum (FWHM) of the main peaks is about (1.8 ± 0.1) eV. The FWHM of the shoulder peaks have very similar values (1.8 ± 0.2) eV. Fitting of the spectra reveals that the shoulder peaks are located at 1.7–1.9 eV higher BE. The intensity of the shoulder peaks varied largely with surface treatment and measurement geometry. The high BE O1s component is stronger in case of grazing detection. These results indicate that the main peaks originate from bulk lattice O and the shoulder peaks from surface O.

Normal surface: There is much debate about the origin of the high BE component in the O1s spectrum from a clean UHV heated α-Al_2O_3 (0001) (1×1) surface. Lazzari and Jupille have addressed this question for long time and suggested that the extra O1s peaks at high BE arise from surface OH groups, which cannot be removed by UHV heating even at high temperature [32,33]. On the other hand, some other results suggest that the α-Al_2O_3 (0001) surfaces heated in vacuum at high temperatures (but below 1200 °C) are terminated by a single Al layer and should be relatively free of hydrogen (see [4] and references therein). As shown in Fig. 1, we also observed the high BE shoulder peaks in O1s spectra after annealing the surfaces in UHV. Compared to the total peak area, the fraction of the area of the shoulder peak is ~10% at grazing detection. We suggest that the high BE O1s component should be ascribed to the topmost O ions sitting just below the terminated Al layer rather than surface OH. This point will be discussed later in detail.

Hydoxylated surface: After exposing the normal surfaces to water, the area of the shoulder peak increases largely to 20% (see Fig. 1). It is well accepted that the α-Al_2O_3 (0001) surface can be extensively hydroxylated via exposure of the surface to water at pressures above 1 Torr [14,15,27–36]. The dissociation of surface adsorbed H_2O molecules produces OH groups bonded with surface Al atoms [14,15]. In photoemission, the surface OH group distinguishes itself by a positive BE shift of O1s relative to the bulk lattice O. This shift, ΔE, varies between 1.3 and 2.0 eV [31–36]. We have observed similar energy shifts of 1.7 to 1.9 eV. Accordingly, it can be concluded that exposure of the surfaces to H_2O effectively produces surface OH groups. The coverage of OH can be estimated by analyzing the ratio

of OH to the total oxygen intensity with a simple inelastic attenuation model [35]. The inelastic mean free path (λ) of O1s photoelectrons was taken as 16.9 Å [47]. This simple calculation results in an OH surface coverage of ∼0.5 ML. The value is similar to that reported by Kelber and coworkers [35,36]. Fluctuations were detected in the OH coverage: typically a value of 0.5 ± 0.1 ML is detected. A large OH coverage, e.g., 1 ML reported by Chambers [34], however, has not been observed.

Hydoxylated surface with O_2 plasma treatment: Exposure of surfaces to water also introduces a small amount of carbon impurities on the surfaces, generally less than 0.05 ML. O_2 plasma treatment can be applied to remove these impurities [34]. Carbon signals were below the detection limit (∼0.01 ML) of our XPS after treating the water-exposed surfaces by O_2 plasma at RT. On the other hand, the shoulder peaks from surface OH were almost unchanged. The OH surface coverage only decreased slightly to 0.47 ML (Fig. 1). Therefore, clean hydroxylated α-Al_2O_3 (0001) surfaces can be obtained via water exposure followed by O_2 plasma treatment at RT.

3.2. The stability of surface OH groups

The above results demonstrate that a well-defined surface preparation process leads to carbon-free OH-terminated surfaces. In the following we will work out at which condition the OH groups can be kept on the surfaces. For that, the stability of surface OH was investigated by exposing the hydroxylated α-Al_2O_3 (0001) surfaces to high temperatures, electron beam illumination, and Ar^+ sputtering.

(i) The effect of heat treatment: The hydroxylated surfaces were step-wise heated in UHV from RT to 900 °C. Every annealing step lasted 12 min, and was followed by XPS measurements at RT. The percentage of the area of the high BE shoulder peak was plotted as a function of annealing temperature (Fig. 2). It can be seen that the intensity of the shoulder peak passes a minimum point: between RT and 500 °C, the intensity decreases with increasing temperature while above 500 °C the peak becomes again stronger with increasing annealing temperature.

The annealing experiments were also conducted at a constant temperature but for different time spans. Again, the fraction of the area of the shoulder peak was plotted as a function of annealing time at 100 °C, 300 °C, 550 °C, and 800 °C (Fig. 3). This area fraction decreased to 13.5%, 8.5%, and 5.8%, after annealing the hydroxylated surfaces at 100 °C, 300 °C, and 550 °C for 20 min, respectively. Subsequently, prolonged heating did not change this area any more. At 800 °C, the area decreased quickly to 6.3% after 10 min annealing, and then increased slowly with increasing annealing time.

Temperatures between RT and 500 °C: The temperature and time dependent experiments (Figs. 2 and 3) clearly show that the area of the shoulder peak keeps on decreasing with increasing temperature from RT to 500 °C. As discussed above, the strong shoulder peaks (∼20%) in O1s spectra, from as-prepared hydroxylated surfaces, originate from surface OH. After annealing at 500 °C the shoulder peak area decreases largely to ∼5%. It is worth mentioning that for the 500 °C annealed surface the intensity of the extra O1s peak does not depend on the detection geometry. This result indicates that there are no surface specific O species, e.g., surface OH groups, on the 500 °C annealed surface anymore. Accordingly, the decrease in the shoulder peak intensity can be explained by the thermal desorption of surface OH. The amount of desorbed OH depends sensitively on annealing temperature but not much on annealing time (see Figs. 2 and 3). The surface OH groups have different binding energies, and the thermal dissociation process is mainly controlled thermodynamically, i.e. by temperature. George and coworkers [28,29] applied

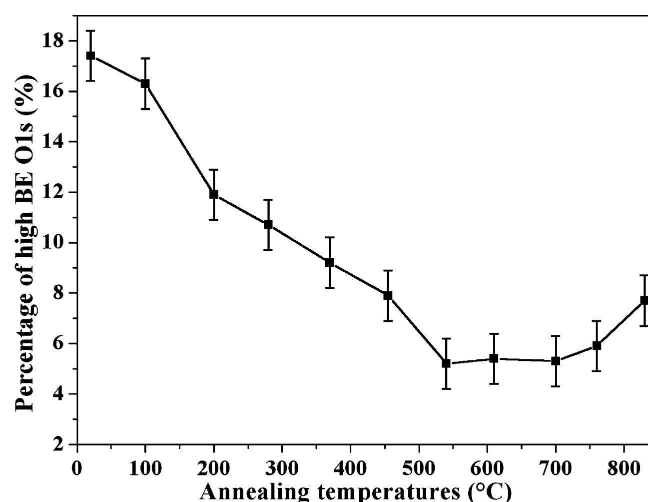

Fig. 2. Fraction (%) of the area of the O1s spectra originating from a high BE component, recorded from a hydroxylated α-Al_2O_3 (0001) surface which was annealed stepwise at different temperatures.

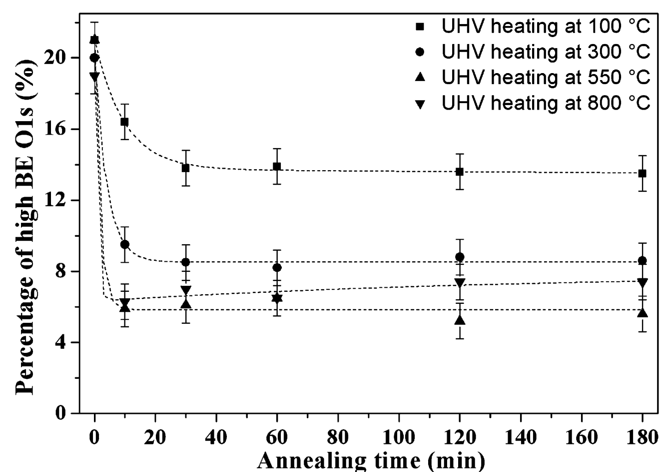

Fig. 3. Fraction (%) of the area of the O1s spectra originating from a high BE component, recorded from a hydroxylated α-Al_2O_3 (0001) surface annealed at 100 °C, 300 °C, 550 °C, and 800 °C for different times, respectively.

thermal desorption techniques to study desorption of H_2O from a hydroxylated α-Al_2O_3 (0001) surface. They observed H_2O desorption over a wide temperature range from RT to 550 K. Lodziana et al. have performed a theoretical investigation of the stability of the hydroxylated α-Al_2O_3 (0001) surface using DFT [48]. These authors demonstrated that an increasing temperature will transform a hydroxylated surface to a clean single Al layer terminated surface. Our XPS data (see Figs. 2 and 3) are quite consistent with these results, suggesting that UHV annealing OH-terminated surfaces results in quick dehydroxylation between RT and 350 °C. All OH has been desorbed below 500 °C, resulting in an Al terminated surface. Compared to the results of Lodziana et al. this desorption temperature range is much wider. They show that desorption of surface OH groups occurs between 400 K and 450 K under UHV conditions. However, we should keep in mind that the model they used described the terraces without any defects. Actually, defects are important centers of hydroxylation. This has been confirmed by SFM experiments [20]. Surface imperfections explain the broad range of desorption energies [48]. Nelson et al. [28] have also discussed the role of different surface defects, e.g., oxygen deficiencies, step edges, and surface Al displacement, in the binding energy of surface hydroxyl groups on the well-defined (1×1) α-Al_2O_3 (0001) surface. The deviation from the perfect Al_2O_3 terrace leads to a range of different binding sites, which can explain the wide H_2O desorption temperature range. The variation of α-Al_2O_3 (0001) surfaces may be attributed to a different thermal stability of surface OH demonstrated in theoretical work and by experimental results from different groups.

Temperatures above 500 °C: Above 500 °C, the intensity of the high BE shoulder peak increases again slightly. The area of the shoulder peak depends on both temperature and time. As shown in Fig. 3, it increases slowly from about 6% to 7.5% with annealing time. After annealing at 900 °C for 2 h, it reached ~10% (Fig. 1). The shoulder peak area depends again on the detection geometry and is larger for grazing detection. Thus, the high BE signals originate from surface O, which appears on the surfaces annealed above 500 °C. In the last paragraph, we have shown that surface OH can be removed almost fully via UHV annealing at 500 °C. Therefore, it seems unlikely to recover the surface OH after annealing an almost OH-free surface at $T > 500$ °C in UHV. This is only possible if the crystal itself acts as a source of hydrogen. However, the hydrogen defect concentration in single crystal α-Al_2O_3 is extremely low (<1 ppm) and the diffusion rate of hydrogen in sapphire is very small [49]. Furthermore, transformation from a clean Al-terminated surface to a hydrated surface necessitates a significant change in chemical potential of H or O [6–8]. However, during annealing in UHV we could not detect a substantial increase of the H_2 or O_2 partial pressures (less than one order of magnitude) for $RT < T < 800$ °C. To our knowledge no experiments have lead to the conclusion that surface OH is generated at high temperatures under UHV conditions. Most of the studies on α-Al_2O_3 (0001) surfaces suggest that the vacuum heated surfaces are rather hydrogen free [4]. There is only one exceptional result reported by Ahn and Rabalais [13]. On the basis of the above discussion one can conclude that the high BE shoulder peak which appears after annealing the sapphire crystals at $T > 500$ °C is not from surface OH, but from, so far unidentified, surface O species which causes a similar O1s chemical shift as surface OH. One possibility how to explain this behavior is to consider a rearrangement of surface atoms or a reconstruction of the surface as we will discuss below.

Clean Al-terminated surfaces are always accompanied by surface relaxations, i.e. an inward relaxation of the first Al layer and outward relaxation of the second O layer. A full relaxation results in almost coplanar Al and O layers and a strong charge redistribution between surface O and Al ions [4–7,13–19]. After relaxation, the surface O definitely has a different chemical environment compared to bulk O. We suggest that the new O1s signals at high BE appearing at $T > 500$ °C are from the surface O caused by a surface relaxation during the heating process of the clean Al-terminated surface. The dependence of the shoulder peak intensity on temperature and time may indicate that the surface relaxation is kinetically controlled. A full relaxation needs high temperatures or long annealing times. Unfortunately, we were not able to detect these relaxations via RHEED measurements.

(ii) Electron beam effect: The hydroxylated surfaces may be subjected to electron-induced surface analysis techniques, e.g., AES, RHEED, etc. To study the influence of electron beam irradiation on the surface OH coverage, the surface was irradiated with different electron beam densities (energy: 4 kV; flux: 0.1 $\mu A/mm^2$, 0.05 $\mu A/mm^2$, and 0.01 $\mu A/mm^2$). The evolution of the intensity of the high BE shoulder peak as a function of illuminating time is shown in Fig. 4. The results indicated that partial surface OH groups were dissociated by the electron beams. The higher the electron flux the stronger the decrease in OH coverage. The sensitivity of surface OH to a large electron beam dose was also observed by other authors [30,50]. These results suggest that electron-excited surface analysis techniques should be carefully applied on the hydroxylated surfaces.

(iii) Ar^+ sputtering effect: We also studied the influence of Ar^+ sputtering on the surface OH coverage. A hydroxylated surface was sputtered with 200 eV Ar^+ for 15 and 30 min, respectively. The O1s spectra were recorded and depicted in Fig. 5. It was shown that the surface OH was almost completely removed after 30 min sputtering. Kelber and coworker reported that only Ar^+ sputtering at energies higher than 2 KeV significantly decreased the surface OH coverage [35,36]. The difference between our results and those from Kelber et al. may come from the different Ar^+ flux, which is also critical besides the Ar^+ energy.

It is worth mentioning that all the dehydroxylated surfaces after electron beam illumination, Ar^+ sputtering, or

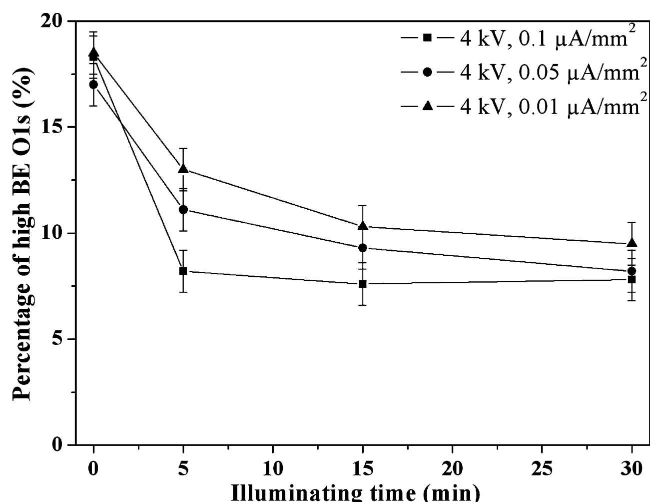

Fig. 4. Fraction (%) of the area of the O1s spectra originating from a high BE component, recorded from a hydroxylated α-Al_2O_3 (0001) surface illuminated by 4 kV electron beam with a flux of 0.1 μA/mm^2, 0.05 μA/mm^2, and 0.01 μA/mm^2 for different times, respectively.

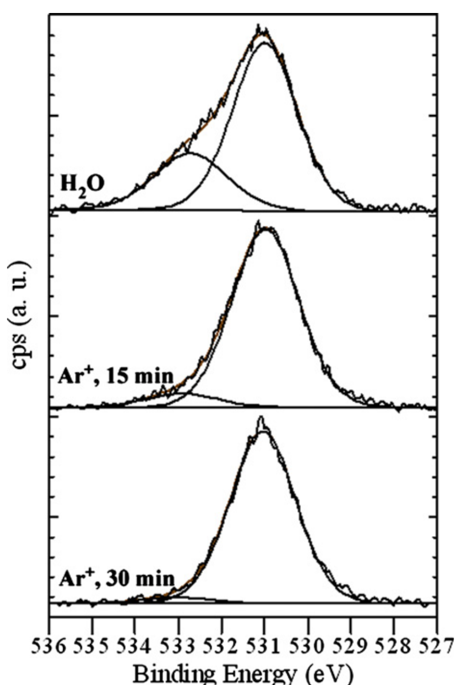

Fig. 5. O1s XPS spectra of a hydroxylated α-Al_2O_3 (0001) surface sputtered at 200 eV Ar^+ for 15 and 30 min.

UHV heating can again recover surface OH groups via exposure to water.

3.3. The interaction of metals with surface OH groups

Three metals, Al, Co, and Cu, with different reactivities, were deposited onto the hydroxylated α-Al_2O_3 (0001) surfaces. Due to the interaction between surface OH groups and metal adatoms [34–38] it is reasonable to assume the layer-like growth of the three metals on the hydroxylated surfaces. The interaction of every metal with surface OH was studied by XPS.

Al/α-Al_2O_3 (0001): Fig. 6 shows the O1s spectra of the hydroxylated Al/α-Al_2O_3 (0001) surface before and after deposition of 1 Å (nominal thickness) Al. It can be seen that the surface OH groups were almost fully dissociated by 1 Å Al. 1 Å Al, which was estimated to be about half a monolayer, has removed the surface OH with a coverage of ~0.5 ML. This result is consistent with the calculation from Wang et al., who reported that one Al monolayer would be sufficient to dissociate all O–H bonds on the fully hydrated surface [51,52]. This process will transfer an OH terminated surface into an Al terminated surface.

For comparison, the normal surface (after UHV heating at 900 °C) subjected to Al adsorption was studied by the same way. Fig. 7 displays the O1s spectra from the normal surface before and after Al deposition. In contrast to the result shown in Fig. 6, the change in the high BE shoulder peak intensity was not significant in case of Al deposition on the normal surface. The XPS results depicted in Fig. 6 has demonstrated that surface OH can be effectively removed by Al adsorption. Therefore, the data in Fig. 7 may present additional evidence that high BE shoulder peaks observed on the normal surfaces could not originate from surface OH but from another surface O species. The interaction between the new surface O and Al is not as strong as that between surface OH and Al (comparing Figs. 6 and 7).

Co/α-Al_2O_3 (0001): Chambers and coworkers have shown laminar growth of ultrathin Co films on hydroxylated α-Al_2O_3 (0001) surfaces [34]. The unusual growth

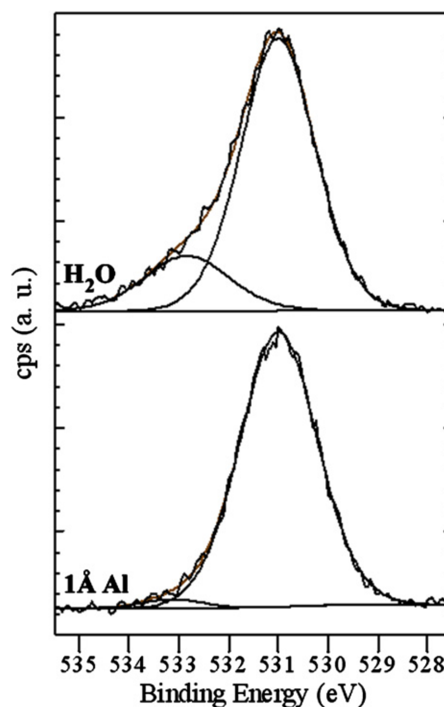

Fig. 6. O1s XPS spectra of a hydroxylated α-Al_2O_3 (0001) surface after deposition of 1 Å Al.

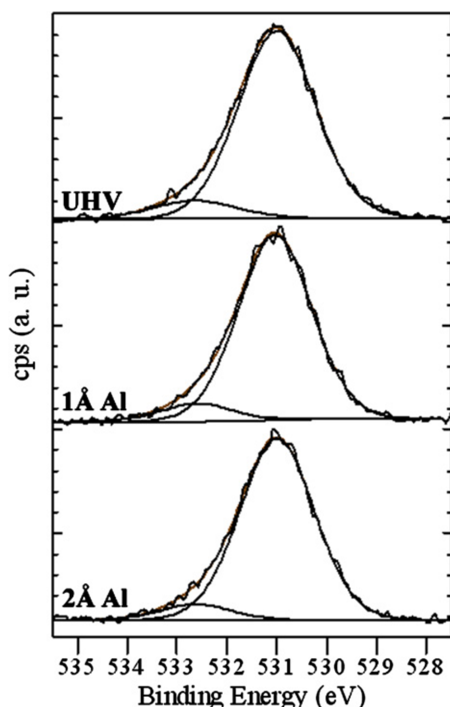

Fig. 7. O1s XPS spectra of a normal α-Al_2O_3 (0001) surface after deposition of 1 Å Al and 2 Å Al.

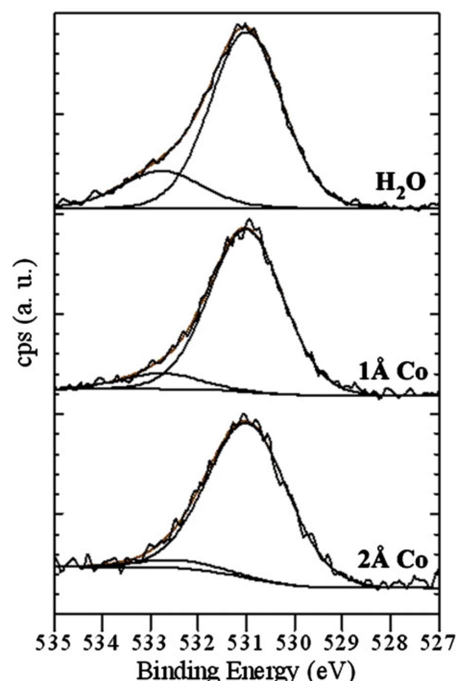

Fig. 8. O1s XPS spectra of a hydroxylated α-Al_2O_3 (0001) surface after deposition of 1 Å Co and 2 Å Co.

behavior was attributed to the strong interaction between Co and the surface. A chemical reaction between Co adatoms and surface OH was confirmed by both experimental and theoretical results. We also observed a strong interaction between Co and a hydroxylated α-Al_2O_3 (0001) surface. The high BE O1s signals were largely attenuated after 2 Å Co deposition (Fig. 8), which resulted from the strong reaction of OH with Co. The slower etching of surface OH by Co compared to Al can be attributed to the lower reactivity of Co to oxygen.

Cu/α-Al_2O_3 (0001): Concerning Cu/α-Al_2O_3 (0001) interfaces, many experimental and theoretical efforts have been devoted to understand the metal-support interaction [35–41]. In particular, the role of surface OH on Cu growth has been studied extensively. Kelber and coworkers applied XPS and DFT calculation to study Cu interactions with hydroxylated α-Al_2O_3 (0001) surfaces [35,36]. It was shown that the presence of surface OH leads to the formation of a Cu(I) monolayer up to 1/3 ML coverage. In agreement with that, recent DFT calculations indicate that at $\theta < 1/3$ ML, Cu atoms can remove surface H and bind the surface through oxygen. This leads to a reduction of hydrogen and formation of Cu(I) [38]. However, Wang et al. [51,52] and Lodziana and Nørskov [43] presented a quite different conclusion on the basis of a weak interaction between Cu and surface OH. These authors conclude that the interfacial OH is stable in the presence of 2 ML Cu, and 1/3 ML H is still present at Cu/sapphire interfaces in the case of thick Cu overlayers [51,52]. We applied XPS to directly monitor the evolution of surface OH as a function of Cu thickness. The O1s spectra in Fig. 9 show that the high BE shoulder peaks decrease slowly with increasing Cu thickness. The O1s results from the hydroxylated and Cu covered surface do not support any strong chemical reactions between surface OH and Cu adatoms. Although a strong influence of surface OH on the Cu film growth, e.g., epitaxy, interfacial bonding, morphology, etc., has

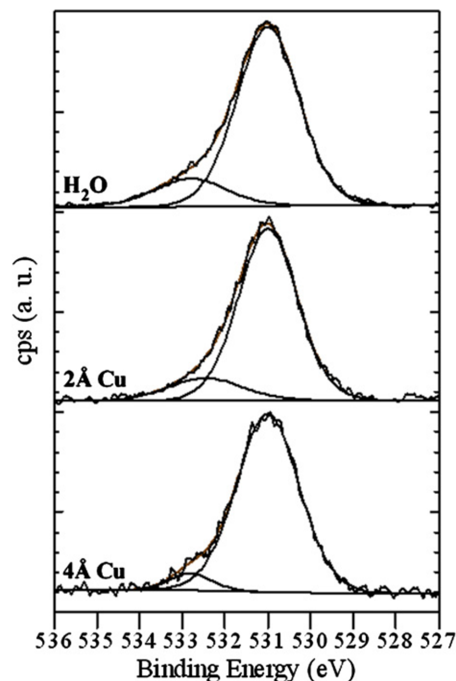

Fig. 9. O1s XPS spectra of a hydroxylated α-Al_2O_3 (0001) surface after deposition of 2 Å Cu and 4 Å Cu.

been observed [35,36,53], the critical role of surface OH in Cu growth can not be simply explained by the interfacial reaction between OH and Cu. One may have to take into account other interaction processes.

4. Conclusion

The hydroxylation of the α-Al_2O_3 (0001) surface can be effectively fulfilled via exposure of the surface to water and O_2 plasma at RT. The resulting surface exhibits an OH coverage of about 0.5 ML. The hydroxylated surfaces are found to be quite sensitive to electron beam illumination, Ar^+ sputtering, high temperature heating, and adsorption of reactive metals:

[1] Ar^+ sputtering at 200 eV with a beam current of 5 mA and a sputtering time of 30 min completely removes surface OH.
[2] A high electron beam density (energy: 4 kV; flux: >0.01 μA/mm^2) partially dissociates the surface OH groups.
[3] Annealing up to 500 °C is sufficient to desorb most of the surface OH groups and results in a clean Al-terminated surface. Annealing at much higher temperature ($T > 500$ °C) leads to the formation of a new surface O species which is related to surface relaxation processes.
[4] Al, Co, and Cu interact differently with surface OH. The higher the reactivity of metals to oxygen (higher oxygen affinity), the stronger the reduction of surface hydrogen via the reaction between metals and surface OH.

Acknowledgements

The authors would like to thank G. Richter, M. Pudleiner for helping in MBE experiments, and E. Tchernychova and S.H. Oh for stimulating discussions.

References

[1] V.E. Henrich, P.A. Cox, The Surface Science of Metal Oxides, Cambridge University Press, Cambridge, 1994.
[2] M. Bäumer, H.-J. Freund, Prog. Surf. Sci. 61 (1999) 127.
[3] R.W.G. Wyckoff (Ed.), Crystal Structures, Krieger, Malabar, 1982.
[4] E.A. Soares, M.A. Van Hove, C.F. Walters, K.F. McCarty, Phys. Rev. B 65 (2002) 195405.
[5] G. Renaud, Surf. Sci. Rep. 32 (1998) 1.
[6] X.G. Wang, A. Chaka, M. Scheffler, Phys. Rev. Lett. 84 (2000) 3650.
[7] R. Di Felice, J.E. Northrup, Phys. Rev. B 60 (1999) R16287.
[8] P.D. Tepesch, A.A. Quong, Phys. Stat. Sol. B 217 (2000) 377.
[9] J. Guo, D.E. Ellis, D.J. Lam, Phys. Rev. B 45 (1992) 13647.
[10] T.J. Godin, J.P. LaFemina, Phys. Rev. B 49 (1994) 7691.
[11] J. Toofan, P.R. Watson, Surf. Sci. 401 (1998) 162.
[12] T. Suzuki, S. Hishita, K. Oyoshi, R. Souda, Surf. Sci. 437 (1999) 289.
[13] J. Ahn, J.W. Rabalais, Surf. Sci. 388 (1997) 121.
[14] K.C. Hass, W.D. Schneider, A. Curioni, W. Andreoni, Science 282 (1998) 265.
[15] K.C. Hass, W.F. Schneider, A. Curioni, W. Andreoni, J. Phys. Chem. B 104 (2000) 5527.
[16] C. Verdozzi, D.R. Jennison, P.A. Schultz, M.P. Sears, Phys. Rev. Lett. 82 (1999) 799.
[17] I. Manassidis, A. De Vita, M.J. Gillan, Surf. Sci. 285 (1993) L517.
[18] V.E. Puchin, J.D. Gale, A.L. Shluger, E.A. Kotomin, J. Günster, M. Brause, V. Kempter, Surf. Sci. 370 (1997) 190.
[19] D.J. Siegel, L.G. Hector Jr., J.B. Adams, Phys. Rev. B 65 (2002) 085415.
[20] C. Barth, M. Reichling, Nature 414 (2001) 54.
[21] G. Renaud, B. Villette, I. Vilfan, A. Bourret, Phys. Rev. Lett. 73 (1994) 1825.
[22] M. Gautier, G. Renaud, L. Pham Van, B. Villette, M. Pollak, N. Thromat, F. Jollet, J.P. Duraud, J. Am. Ceram. Soc. 77 (1994) 323.
[23] T.M. French, G.A. Somorjai, J. Phys. Chem. 74 (1970) 2489.
[24] M. Vermeersch, F. Malengreau, R. Sporken, R. Caudano, Surf. Sci. 323 (1995) 175.
[25] M.A. Nygren, D.H. Gay, C.R.A. Catlow, Surf. Sci. 380 (1997) 113.
[26] J.M. Wittbrodt, W.L. Hase, H.B. Schlegel, J. Phys. Chem. B 102 (1998) 6539.
[27] P.J. Eng, T.P. Trainor, G.E. Brown Jr., G.A. Waychunas, M. Newville, S.R. Sutton, M.L. Rivers, Science 288 (2000) 1029.
[28] C.E. Nelson, J.W. Elam, M.A. Cameron, M.A. Tolbert, S.M. George, Surf. Sci. 416 (1998) 341.
[29] J.W. Elam, C.E. Nelson, M.A. Cameron, M.A. Tolbert, S.M. George, J. Phys. Chem. B 102 (1998) 7008.
[30] V. Coustet, J. Jupille, Surf. Sci. 307–309 (1994) 1161.
[31] P. Liu, T. Kendelewicz, G.E. Brown Jr., E.J. Nelson, S.A. Chambers, Surf. Sci. 417 (1998) 53.
[32] R. Lazzari, J. Jupille, Phys. Rev. B 71 (2005) 045409.
[33] R. Lazzari, J. Jupille, Surf. Sci. 507–510 (2002) 683.
[34] S.A. Chambers, T. Droubay, D.R. Jennison, T.R. Mattsson, Science 297 (2002) 827.
[35] J.A. Kelber, C. Niu, K. Shepherd, D.R. Jennison, A. Bogicevic, Surf. Sci. 446 (2000) 76.
[36] C. Niu, K. Shepherd, D. Martini, J. Tong, J.A. Kelber, D.R. Jennison, A. Bogicevic, Surf. Sci. 465 (2000) 163.
[37] N.C. Hernández, J.F. Sanz, J. Phys. Chem. B 106 (2002) 11495.
[38] J.F. Sanz, N.C. Hernández, Phys. Rev. Lett. 94 (2005) 016104.
[39] C. Scheu, Interface Sci. 12 (2004) 127.
[40] M. Gautier, J.P. Duraud, L. Pham Van, Surf. Sci. 249 (1991) L327.
[41] S. Varma, G.S. Chottiner, M. Arbab, J. Vac. Sci. Technol. A 10 (1992) 2857.
[42] W. Zhang, J.R. Smith, Phys. Rev. B 61 (2000) 16883.
[43] Z. Lodziana, J.K. Nørskov, J. Chem. Phys. 115 (2001) 11261.
[44] T. Akatsu, C. Scheu, T. Wagner, T. Gemming, N. Hosoda, T. Suga, M. Rühle, Appl. Surf. Sci. 165 (2000) 159.
[45] D. Briggs, M.P. Seah, Practical Surface Analysis by Auger and X-ray Photoelectron Spectroscopy, John Wiley, Chichester, 1990.
[46] J. Moulder, W.F. Stickle, P.E. Sobol, K.D. Bomben, The Handbook of the X-ray Photoelectron Spectroscopy, Pekin-Elmer Corporation, 1992.
[47] S. Tanuma, C.J. Powell, D.R. Penn, Surf. Interface Anal. 17 (1991) 927.
[48] Z. Lodziana, J.K. Nørskov, P. Stoltze, J. Chem. Phys. 118 (2003) 11179.
[49] A.K. Kronenberg, J. Castaing, T.E. Mitchell, S.H. Kirby, Acta Mater. 48 (2000) 1481.
[50] J.G. Chen, J.E. Crowell, J.T.J. Yates, J. Chem. Phys. 84 (1986) 5906.
[51] X.G. Wang, J.R. Smith, M. Scheffler, Phys. Rev. B 66 (2002) 073411.
[52] X.G. Wang, J.R. Smith, J. Am. Ceram. Soc. 86 (2003) 696.
[53] S.H. Oh, C. Scheu, T. Wagner, E. Tchernychova, M. Rühle, Acta Mater. 54 (2006) 2685.